Cardiovascular Research (2010) **86**, 82–91
doi:10.1093/cvr/cvp396

Measuring intracellular pH in the heart using hyperpolarized carbon dioxide and bicarbonate: a ^{13}C and ^{31}P magnetic resonance spectroscopy study

Marie A. Schroeder[1]*, Pawel Swietach[2], Helen J. Atherton[1], Ferdia A. Gallagher[3,4], Phillip Lee[1], George K. Radda[1], Kieran Clarke[1], and Damian J. Tyler[1]

[1]Cardiac Metabolism Research Group, Department of Physiology, Anatomy and Genetics, University of Oxford, Sherrington Building, Parks Road, Oxford OX1 3PT, UK; [2]Proton Transport Group, Department of Physiology, Anatomy and Genetics, University of Oxford, Sherrington Building, Parks Road, Oxford OX1 3PT, UK; [3]Department of Radiology, University of Cambridge, Addenbrooke's Hospital, Cambridge CB2 2QQ, UK; and [4]CRUK Cambridge Research Institute, Cambridge CB2 0RE, UK

Received 16 October 2009; revised 29 November 2009; accepted 10 December 2009; online publish-ahead-of-print 15 December 2009

Time for primary review: 16 days

Aims Technological limitations have restricted *in vivo* assessment of intracellular pH (pH_i) in the myocardium. The aim of this study was to evaluate the potential of hyperpolarized [1-^{13}C]pyruvate, coupled with ^{13}C magnetic resonance spectroscopy (MRS), to measure pH_i in the healthy and diseased heart.

Methods and results Hyperpolarized [1-^{13}C]pyruvate was infused into isolated rat hearts before and immediately after ischaemia, and the formation of $^{13}CO_2$ and $H^{13}CO_3^-$ was monitored using ^{13}C MRS. The HCO_3^-/CO_2 ratio was used in the Henderson–Hasselbalch equation to estimate pH_i. We tested the validity of this approach by comparing ^{13}C-based pH_i measurements with ^{31}P MRS measurements of pH_i. There was good agreement between the pH_i measured using ^{13}C and ^{31}P MRS in control hearts, being 7.12 ± 0.10 and 7.07 ± 0.02, respectively. In reperfused hearts, ^{13}C and ^{31}P measurements of pH_i also agreed, although ^{13}C equilibration limited observation of myocardial recovery from acidosis. In hearts pre-treated with the carbonic anhydrase (CA) inhibitor, 6-ethoxyzolamide, the ^{13}C measurement underestimated the ^{31}P-measured pH_i by 0.80 pH units. Mathematical modelling predicted that the validity of measuring pH_i from the $H^{13}CO_3^-/^{13}CO_2$ ratio depended on CA activity, and may give an incorrect measure of pH_i under conditions in which CA was inhibited, such as in acidosis. Hyperpolarized [1-^{13}C]pyruvate was also infused into healthy living rats, where *in vivo* pH_i from the $H^{13}CO_3^-/^{13}CO_2$ ratio was measured to be 7.20 ± 0.03.

Conclusion Metabolically generated $^{13}CO_2$ and $H^{13}CO_3^-$ can be used as a marker of cardiac pH_i *in vivo*, provided that CA activity is at normal levels.

Keywords Magnetic resonance spectroscopy • Hyperpolarization • pH • Ischaemia • Carbonic anhydrase

1. Introduction

The rapid onset of acidosis is a well-documented characteristic of myocardial ischaemia.[1,2] Under poor coronary perfusion, anaerobic glycolysis increases in the heart, producing intracellular protons and lactic acid that accumulate in the intra- and extracellular spaces.[3] Some of the acid reacts with HCO_3^- to form CO_2, which adds to any CO_2 generated by residual oxidative metabolism. Accumulation of protons, lactic acid, and CO_2 in the ischaemic heart decreases intracellular pH (pH_i) from normal levels of around 7.1–7.2.[1,2] Transient acidosis during ischaemia may be beneficial, as it decreases the major adenosine triphosphate (ATP) consumer, contractility, and thus conserves ATP for ion transport.[4] However, the ATP reduction caused by severe and sustained ischaemia decreases Na^+,K^+-ATPase activity, which increases myocardial Na^+ levels. Increased Na^+ inhibits Ca^{2+} extrusion via the Na^+/Ca^{2+} exchanger, thus elevating myocardial Ca^{2+} and damaging the myocardium.[5]

* Corresponding author. Tel: +44 1865 282249; fax: +44 1865 282272, Email: marie.schroeder@dpag.ox.ac.uk

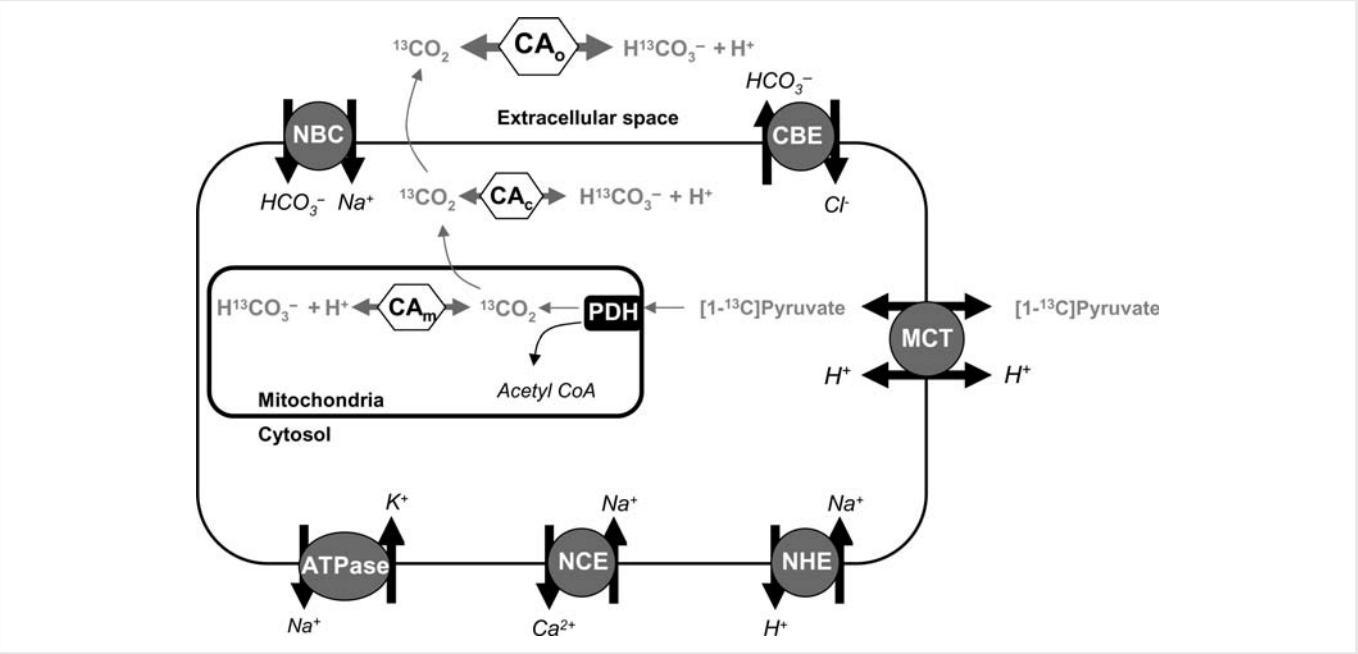

Figure 1 The metabolic fate of infused hyperpolarized [1-^{13}C]pyruvate is shown. Infused pyruvate is oxidized to form acetyl-CoA and the by-product, $^{13}CO_2$, in the mitochondria, by the enzyme PDH. Mitochondrial $^{13}CO_2$ is then thought to rapidly diffuse into the cytosol, and subsequently out of the cell. In theory, $^{13}CO_2$ in either the mitochondria or the cytosol could equilibrate with $H^{13}CO_3^-$, mediated by CA activity. Once $^{13}CO_2$ diffuses into the bloodstream, it will rapidly equilibrate with $H^{13}CO_3^-$ via CA. CA, carbonic anhydrase; PDH, pyruvate dehydrogenase; MCT, mono-carboxylate transporter; NHE, sodium proton exchanger; NBC, sodium bicarbonate carrier; CBE, chloride bicarbonate exchanger; NCE, sodium calcium exchanger.

^{31}P magnetic resonance spectroscopy (MRS) has long been the gold standard for pH_i measurement in the isolated perfused heart,[6] based on the chemical shift of the inorganic phosphate (P_i) peak.[7,8] However, ^{31}P MRS cannot measure cardiac pH_i *in vivo*, because 2,3-diphosphoglycerate (2,3-DPG) in the ventricular blood contaminates the myocardial P_i peak.[6,9,10]

The pH-dependent equilibrium between bicarbonate and CO_2 has been used to measure extracellular pH (pH_o) non-invasively in tumours.[11] By infusing hyperpolarized ^{13}C-bicarbonate intravenously, MR was used to image the distribution of hyperpolarized bicarbonate and CO_2 and a pH map was generated using the Henderson–Hasselbalch equation:

$$\mathrm{pH} = \mathrm{p}K_a + \log\left(\frac{[HCO_3^-]}{[CO_2]}\right) \quad (1)$$

where pK_a is the acid-dissociation constant of CO_2, which is 6.15 in the Krebs–Henseleit buffer.[12]

For correct application of the Henderson–Hasselbalch equation, the following two conditions must be met:

(i) $^{13}CO_2$ to $H^{13}CO_3^-$ exchange kinetics, catalysed by carbonic anhydrase (CA), must be rapid and
(ii) $^{13}CO_2$ and $H^{13}CO_3^-$ signals must be detected simultaneously from the same cellular compartment.

In tumours, the Henderson–Hasselbalch equation was applied correctly because of the high CA activity on the surface of tumour cells[13] and within erythrocytes,[14] and the slow, transporter-mediated, cellular uptake of infused bicarbonate.[15]

A similar approach may be useful for measuring pH_i in the *in vivo* heart.[16,17] Infusion of hyperpolarized [1-^{13}C]pyruvate results in mitochondrial production of hyperpolarized $^{13}CO_2$ by pyruvate dehydrogenase (PDH, *Figure 1*).[18] Hyperpolarization by the dynamic nuclear polarization method increases the ^{13}C MR sensitivity of pyruvate, and other ^{13}C-labelled metabolites, more than 20 000-fold.[19] Further, when a hyperpolarized metabolite is infused into tissue, the high-sensitivity ^{13}C label is transferred to the tracer's metabolic products, enabling unprecedented real-time visualization of the biochemical mechanisms of normal and abnormal metabolism. Only metabolic processes that occur rapidly can be monitored using hyperpolarized ^{13}C MR methods because the hyperpolarized signal decays to thermal equilibrium according to its inherent spin–lattice relaxation time (in the case of [1-^{13}C]pyruvate with a time constant of 50–60 s).

In theory, simultaneous detection of hyperpolarized [1-^{13}C]pyruvate-derived $^{13}CO_2$ and $H^{13}CO_3^-$ could be used to measure pH_i. However, in cardiac myocytes, the conditions required for the correct use of the Henderson–Hasselbalch equation may not apply. As shown in *Figure 1*, metabolically generated CO_2 diffuses rapidly from its site of production into the cytosol, and subsequently into the extracellular space.[20] Cardiac myocytes also have HCO_3^- transport activity, through proteins such as the Na^+–HCO_3^- co-transporter and the Cl^-/HCO_3^- exchanger.[12] Studies of CA localization and kinetics in cardiac myocytes suggest low intracellular CA activity.[21] Under the acidic conditions, typical of ischaemia, CA activity is expected to be even lower.[22,23] Further, PDH flux post-ischaemia must be sufficiently high to enable MR detection of $^{13}CO_2$ and $H^{13}CO_3^-$ prior to decay of the hyperpolarized ^{13}C MR signal.

The aim of the present study was to evaluate the potential of hyperpolarized ^{13}C MR for the non-invasive measurement of pH_i in the heart. We measured PDH flux and the production of $^{13}CO_2$ and $H^{13}CO_3^-$ in isolated hearts before and after ischaemia and with CA activity inhibited. We used mathematical modelling to determine whether, and under what conditions, the $H^{13}CO_3^-/^{13}CO_2$ ratio could be used to measure cardiac pH_i. Finally, we measured pH_i in the *in vivo* rat heart.

2. Methods

2.1 The isolated perfused rat heart

All investigations conformed to the Guide for the Care and Use of Laboratory Animals published by the US National Institutes of Health (NIH Publication No. 85-23, revised 1996), the Home Office Guidance on the Operation of the Animals (Scientific Procedures) Act, 1986 (HMSO), and to institutional guidelines. Male Wistar rats (~300 g) were anaesthetized using a 0.7 mL ip injection of pentobarbital sodium (200 mg/mL Euthatal). The beating hearts were quickly removed and arrested in the ice-cold Krebs–Henseleit perfusion buffer, and the aorta was cannulated for perfusion in recirculating retrograde Langendorff mode at a constant 85 mmHg pressure and 37°C temperature.[24] The Krebs–Henseleit bicarbonate perfusion buffer contained 1.2 mM inorganic phosphate (KH_2PO_4), 11 mM glucose, and 2.5 mM pyruvate and was aerated with a mixture of 95% oxygen (O_2) and 5% carbon dioxide (CO_2) to give a final pH of 7.4 at 37°C. The broad-spectrum CA inhibitor, 6-ethoxyzolamide (ETZ), was dissolved in dimethyl sulfoxide (DMSO) and added to the perfusate to achieve a final concentration of 100 μM (with DMSO < 0.01% of total buffer volume). ETZ was expected to evenly distribute throughout the intra- and extracellular spaces to inhibit all cardiac CA isoforms.[20] Unless specified, compounds were obtained from Sigma (Gillingham, UK). For further details of the Langendorff heart perfusion method, see Supplementary material online, *S1*.

2.2 Experimental protocols

2.2.1 Control protocol

Isolated hearts ($n = 6$) were perfused for ~30 min at 85 mmHg. For the initial 20 min, ^{31}P MRS was used to measure pH_i. After this, hyperpolarized [1-^{13}C]pyruvate was infused and the progress of ^{13}C-labelled compounds was followed using ^{13}C MRS.

2.2.2 Inhibition of CA

Hearts ($n = 5$) were perfused for ~30 min. After 10 min of perfusion in normal buffer, the hearts were switched to buffer containing 100 μM ETZ. ^{31}P MRS was performed for 20 min (10 min before and 10 min after switch over to ETZ-containing buffer). Ten minutes after the start of ETZ perfusion, hyperpolarized [1-^{13}C]pyruvate was infused and MRS was switched from ^{31}P to ^{13}C.

2.2.3 Reperfusion following ischaemia

Hearts ($n = 12$) were perfused for ~30 min, followed by 10 min of total, global ischaemia, and 15 min reperfusion. ^{31}P MRS spectra were acquired for 20 min immediately before and 9 min during ischaemia. Hyperpolarized [1-^{13}C]pyruvate was infused immediately after ischaemia, such that hearts were reperfused with hyperpolarized tracer. In some hearts ($n = 6$), ^{31}P MRS was performed throughout the reperfusion period. In other hearts ($n = 6$), ^{13}C MRS was performed for 2 min during initial reperfusion with hyperpolarized [1-^{13}C]pyruvate, followed by 10 min of ^{31}P MR spectral acquisition. For details of the [1-^{13}C]pyruvate preparation and delivery, see Supplementary material online, *S2*.

2.3 Magnetic resonance spectroscopy

^{31}P MR spectra were acquired at 202.5 MHz using a 30° radiofrequency (RF) pulse and a repetition delay of 0.25 s. The phosphocreatine (PCr) resonance was set at 0 ppm and the chemical shifts of all peaks were referenced to that of PCr. Each spectrum consisted of 120 transients, giving a total acquisition time of 30 s. As these partially saturated spectra had shorter repetition times than the longitudinal relaxation time of ^{31}P nuclei, an unsaturated spectrum was initially acquired from the hearts using a 90° pulse with repetition time of 15 s and 40 transients, and an acquisition time of 10 min. The unsaturated spectra were used to correct metabolite concentrations for the effects of saturation.

Acquisition of ^{13}C MR spectra commenced immediately after infusion of hyperpolarized [1-^{13}C]pyruvate and [1-^{13}C]pyruvate infusion continued throughout acquisition. Spectra were acquired with 1 s temporal resolution over 2 min (excitation flip angle = 30°, 120 acquisitions). Spectra were centred at 150 ppm and referenced to the [1-^{13}C]pyruvate resonance at 171 ppm, and 4096 points were acquired over a bandwidth of 100 ppm.

In vivo hyperpolarized [1-^{13}C]pyruvate MRS experiments were performed as described previously.[18] Briefly, [1-^{13}C]pyruvic acid was hyperpolarized and dissolved/neutralized in a prototype ^{13}C polariser system.[25] Each living rat ($n = 6$) was positioned at the isocentre of a 7 T Varian horizontal bore MR scanner, with a dual-tuned $^{1}H/^{13}C$ coil localized over the animal's chest. Aqueous hyperpolarized [1-^{13}C]pyruvate (80 μmol) was then infused into a living rat via the tail vein over 10 s, and cardiac ^{13}C spectra were acquired with a low 7.5° flip angle every second for 1 min. For further details of *in vivo* hyperpolarized [1-^{13}C]pyruvate MRS experiments, refer to Supplementary material online, *S3*.

2.4 Data analysis

2.4.1 Carbon-13

Cardiac ^{13}C MR spectra were analysed using the AMARES algorithm, as implemented in the jMRUI software package.[26] Spectra were DC offset corrected based on the last half of acquired points and peaks corresponding with [1-^{13}C]pyruvate and its metabolic derivatives were fitted assuming a Lorentzian line shape, initial peak frequencies, relative phases, and linewidths.

For spectra acquired from perfused rat hearts, the maximum peak area of each metabolite over the 2 min of acquisition was determined for each series of spectra and expressed as a percentage of the maximum [1-^{13}C]pyruvate resonance.[18] The rate of signal production for each metabolite, in percent per second (%/s), was measured as the slope of the mean metabolite increase over the first 5 s following its appearance, over which time the metabolite signal increased linearly. Additionally, a first-order exponential signal decay term was fit to each metabolite peak from the point of maximum signal over the course of signal decay. Decay of the hyperpolarized signal depends on the intrinsic spin–lattice relaxation of the nucleus, production and consumption rates of the metabolite, and metabolite washout, and may therefore provide information about metabolite accumulation in the states of no-flow ischaemia and CA inhibition.

Average time courses for $H^{13}CO_3^-$, $^{13}CO_2$, and their sum were calculated for all hearts for further data analysis. $H^{13}CO_3^-$ plus $^{13}CO_2$, normalized to the maximum pyruvate peak area to allow for any differences in polarization, was used as a qualitative indicator of PDH flux. The average $H^{13}CO_3^-$ and $^{13}CO_2$ time courses were inserted into an applied form of the Henderson–Hasselbalch equation:

$$pR = 6.15 + \log\left(\frac{[H^{13}CO_3^-]}{[^{13}CO_2]}\right) \quad (2)$$

The output of Eq. (2) is a variable pR which should, under the two conditions outlined in Section 1, measure pH. Upon the initial arrival of [1-^{13}C]pyruvate, the relative proportions of $^{13}CO_2$ and $H^{13}CO_3^-$ (and thus pR) equilibrated over several seconds to reach a

steady-state value. The calculated pR was fit to a first-order exponential equation to determine the steady-state value and time constant.

2.4.2 Phosphorus-31

Cardiac ^{31}P MR spectra were analysed using the AMARES algorithm in the jMRUI software package.[26] Spectra were corrected for DC offset using the last half of acquired points. The PCr, P_i, α-, β-, and γ-ATP resonances were fitted assuming a Lorentzian line shape, peak frequencies, relative phases, linewidths, and J-coupling parameters. pH_i was calculated from the P_i chemical shift.[8,27] Absolute ^{31}P metabolite concentrations were calculated using an ATP concentration of 10.6 mM from the first γ-ATP peak area[28] and expressing all other ATP and PCr peak areas relative to this area.[27]

2.4.3 Modelling

A system of ordinary differential equations was formulated to test the suitability of using the CO_2–HCO_3^- equilibrium to measure pH_i. For details of the mathematical model, see Supplementary material online, *S4*.

2.4.4 Statistical methods

Data are given as mean ± standard error. Statistical significances between pre- and post-ischaemic groups, and pre-ischaemic and ETZ-perfused groups, were assessed using a paired Student's *t*-test. Statistical significance was considered at $P < 0.05$.

3. Results

3.1 Myocardial energetics

Cardiac function and ^{31}P MR spectra were characteristic of the isolated rat heart during pre-ischaemia, ischaemia, and reperfusion.[1] A description of cardiac function throughout the protocol and an example of a ^{31}P spectrum of a heart before ischaemia are shown in Supplementary material online, *S5*. Pre-ischaemia, the average [ATP] was 10.6 ± 0.7 mM and [PCr] was 19.7 ± 0.9 mM (*Figure 2*). Two minutes after stopping coronary flow, [PCr] decreased to 3.2 mM, to remain at 1.1–2.1 mM for the remainder of ischaemia. The rate of [ATP] hydrolysis during ischaemia was 0.14 ± 0.10 mM/min. Five minutes after reperfusion, PCr had recovered to 17.6 ± 1.9 mM, whereas ATP remained at 8.2 ± 2.5 mM.

Perfusion with ETZ had no effect on [ATP] or [PCr] throughout the perfusion protocol (data not shown). Prior to ETZ perfusion, hearts had an average PCr of 17.8 ± 1.9 mM and ATP of 10.6 ± 0.5 mM. During ETZ perfusion, the average [PCr] was 18.0 ± 1.5 mM and [ATP] was 10.3 ± 0.9 mM.

3.2 PDH flux

A representative spectrum of [1-^{13}C]pyruvate in the perfused heart, and the typical kinetic progression of [1-^{13}C]pyruvate metabolites, is shown in *Figure 3*. Following infusion of [1-^{13}C]pyruvate into control hearts, [1-^{13}C]lactate (183.2 ppm), $H^{13}CO_3^-$ (160.9 ppm), and [1-^{13}C]alanine (176.5 ppm) were clearly detectable with high signal compared with the baseline. A resonance corresponding to $^{13}CO_2$ was also visible, with 1 s temporal resolution, at a chemical shift of 124.5 ppm. The initial rates of production and the maximum peak areas for the [1-^{13}C]pyruvate-derived metabolites, in pre-ischaemic, ETZ, and reperfused hearts, are given in *Table 1*.

The maximum peak areas of $H^{13}CO_3^-$, $^{13}CO_2$, and their sum were not significantly different from baseline when [1-^{13}C]pyruvate was infused into the myocardium upon reperfusion. However, the initial rate of $H^{13}CO_3^-$ plus $^{13}CO_2$ production was 54% slower upon reperfusion, compared with the pre-ischaemic myocardium, as indicated by the slope of the reperfusion peaks shown in *Figure 4*. Additionally, the decay rate of hyperpolarized $^{13}CO_2$ signal was 30% faster in reperfused hearts than in pre-ischaemic hearts ($P < 0.001$), indicating enhanced CO_2 washout upon re-flow after ischaemia.

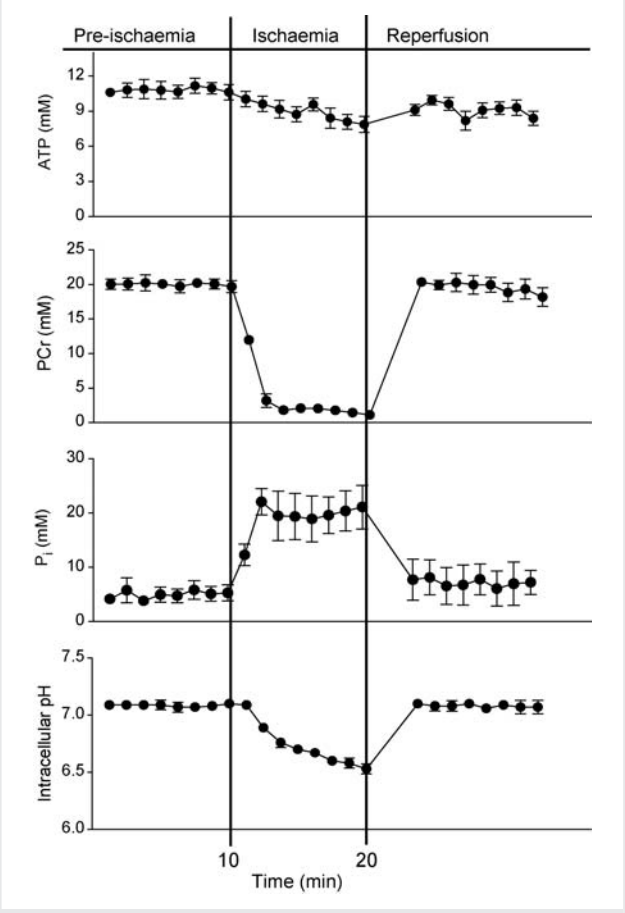

Figure 2 Changes in ATP, PCr, P_i, and pH_i, before, during, and after ischaemia. ATP levels gradually decreased during ischaemia, and after reperfusion, partially recovered to pre-ischaemia levels. PCr levels rapidly decreased at the onset of ischaemia and rapidly recovered to pre-ischaemic levels after reperfusion. P_i levels rapidly increased at the onset of ischaemia and rapidly decreased to pre-ischaemic levels after reperfusion. pH_i gradually decreased from 7.07 to 6.49 during ischaemia and rapidly recovered to pre-ischaemia levels following reperfusion.

ETZ had no significant effect on the initial rate of $H^{13}CO_3^-$ plus $^{13}CO_2$ production, or the maximum peak area of the sum of $H^{13}CO_3^-$ and $^{13}CO_2$, compared with pre-ischaemic hearts (*Figure 4*). However, ETZ increased the maximum $^{13}CO_2$ peak area by four-fold, whereas decreasing the maximum $H^{13}CO_3^-$ peak area by two-fold (*Table 1*, $P < 0.001$). Additionally, the decay rate of hyperpolarized $^{13}CO_2$ signal was 19% faster in reperfused hearts than in pre-ischaemic hearts ($P < 0.05$), possibly indicating enhanced CO_2 diffusion out of myocytes in the absence of CA activity.

3.3 Measurement of pH_i in the isolated perfused heart

Figure 5A shows the changes in $H^{13}CO_3^-$ and $^{13}CO_2$, both normalized to the maximum [1-^{13}C]pyruvate signal, which were used for the

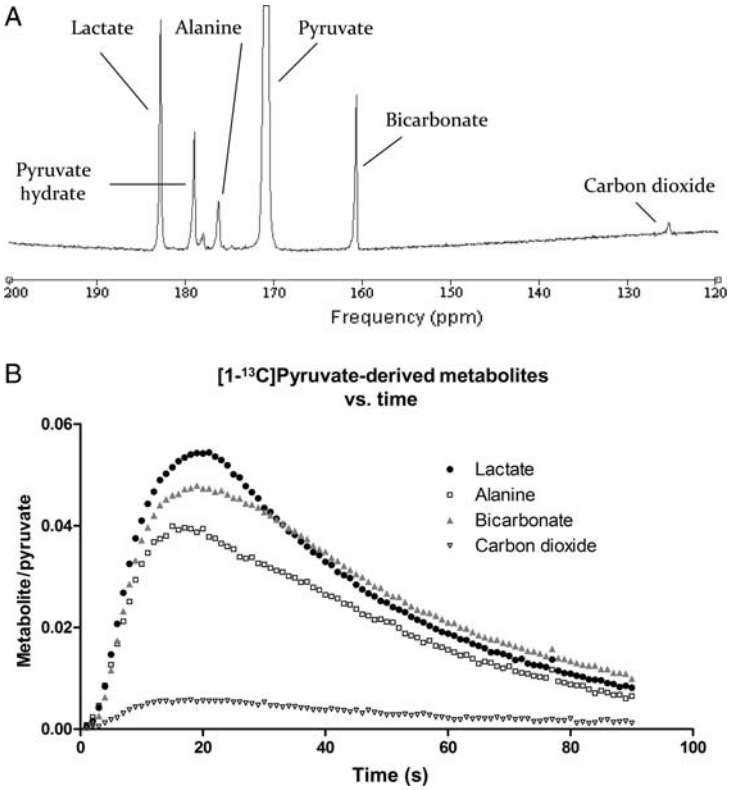

Figure 3 (*A*) Representative spectrum acquired during hyperpolarized [1-^{13}C]pyruvate infusion into the isolated perfused heart. Five single 1 s spectra were summed to yield this spectrum, acquired using a 30° RF pulse. (*B*) Changes in the metabolic products of [1-^{13}C]pyruvate in pre-ischaemic hearts ($n = 6$).

calculation of pR. When hyperpolarized [1-^{13}C]pyruvate reached the isolated heart, metabolically generated $H^{13}CO_3^-$ and $^{13}CO_2$ were out of equilibrium for ~5 s before pR [Eq. (2)] reached a steady-state value of 7.12 ± 0.10 (*Figure 5B*). Fully relaxed ^{31}P measurements, acquired in the pre-ischaemic heart, gave a pH_i of 7.07 ± 0.02. The pH_i measured using ^{31}P MRS and the 95% confidence interval are overlaid on the ^{13}C results in *Figure 5B*.

^{31}P MRS confirmed that CA inhibition with ETZ had no effect on steady-state myocardial pH_i (pH_i of 7.02 ± 0.03 before ETZ treatment and 7.00 ± 0.04 after ETZ treatment). Perfusion with [1-^{13}C]pyruvate and ETZ generated more $^{13}CO_2$ than $H^{13}CO_3^-$ (*Figure 5C*) with no change in total $H^{13}CO_3^-$ plus $^{13}CO_2$. The pR, calculated from the $H^{13}CO_3^-/CO_2$ ratio, stabilized within 20 s to a steady-state pR of 6.21 ± 0.13 (*Figure 5D*). Thus, inhibition of CA activity slowed CO_2–HCO_3^- conversion, as shown by the lengthening of the out-of-equilibrium period, but also by the steady-state pR which was 0.79 pH units below the pH_i measured using ^{31}P MRS.

In reperfused hearts, ^{31}P MRS revealed that pH_i recovered from a value of 6.49 ± 0.04 at the end of ischaemia to 7.04 ± 0.13, at a rate of 0.73 pH units/min during the 45 s immediately after reflow (*Figure 6*). In hearts reperfused with hyperpolarized [1-^{13}C]pyruvate, the pR from the $H^{13}CO_3^-/CO_2$ ratio was the same as pH_i from ^{31}P MRS after 15 s of reperfusion, when averaged into 30 s segments that corresponded with acquisition of ^{31}P spectra. After 45 and 75 s, both ^{13}C and ^{31}P measurements gave almost identical pH_i measurements (^{13}C: 7.01 ± 0.01 at 45 s and 6.98 ± 0.02 at 75 s; ^{31}P: 7.04 ± 0.13 at 45 s and 7.00 ± 0.04 at 75 s, *Figure 6*).

3.4 Mathematical modelling of experimental results

Results of the mathematical model of $^{13}CO_2$ production, efflux, and hydration to $H^{13}CO_3^-$ by CA are depicted in *Figure 7*. *Figure 7A* shows the output of the model that best-fits the experimental data presented in *Figure 5*. Constants K_{CO_2} ($10^{-6.15}$ M), k_f (0.14 s^{-1}), and k_r (k_f/K_{CO_2}) were obtained from published values[21] and other parameters were obtained by least-squares fitting: P_{pyr} (0.2 s^{-1}), P_{CO_2} (0.2 s^{-1}), ρ (0.006 s^{-1}), α (1/33 s for pyruvate, 1/6 s for CO_2 and HCO_3^-). The best simulation of our experimental $^{13}CO_2$ and $H^{13}CO_3^-$ results (*Figure 7A*) indicated that CA activity (γ) enhanced the conversion rate of $^{13}CO_2$ into $H^+ + H^{13}CO_3^-$ by 10-fold in pre-ischaemic hearts. This value was in line with an *in vitro* study that reported CA-enhanced CO_2 hydration by five-fold in isolated myocytes.[21]

Figure 7B shows the value of pR [Eq. (2)] derived from the simulations in *Figure 7A*. At normal CA activity ($\gamma = 10$), pR approached 6.8 within 17 s, giving a reasonable approximation to the real pH_i of 7.1. However, in the absence of CA activity ($\gamma = 1$), pR approached a significantly lower asymptote of 6.1 within 24 s.

Apart from CA activity, another factor that can disturb the equilibrium between H^+, HCO_3^- and CO_2 is HCO_3^- transport. *Figure 7C* and *D* illustrates the implications of HCO_3^- extrusion and uptake, respectively, on the steady-state value of pR. In the presence of ± 5 mM/min transmembrane HCO_3^- flux, the value of pR was not greatly altered, compared with a model with no net HCO_3^- transport.

Table 1 Metabolite levels and kinetic parameters from ^{13}C MR spectra in pre-ischaemia, reperfused, and ETZ-perfused isolated hearts

	[1-^{13}C]Lactate			[1-^{13}C]Alanine		
	Pre-ischaemia	**Reperfusion**	**ETZ**	**Pre-ischaemia**	**Reperfusion**	**ETZ**
Maximum metabolite/pyruvate (%)	6 ± 1	31 ± 3†	7 ± 2	4.2 ± 0.3	3.5 ± 0.2	5.7 ± 0.4
Initial production rate (%/s)	0.7 ± 0.1	4.4 ± 0.4†	0.7 ± 0.2	0.43 ± 0.09	0.28 ± 0.03	0.7 ± 0.01
Decay, τ (s)	35 ± 4	22.3 ± 0.2*	41 ± 5	39 ± 2	41 ± 1	43 ± 7
	$H^{13}CO_3^-$			$^{13}CO_2$		
	Pre-ischaemia	**Reperfusion**	**ETZ**	**Pre-ischaemia**	**Reperfusion**	**ETZ**
Maximum metabolite/pyruvate (%)	4.7 ± 0.6	3.8 ± 0.4	2.1 ± 0.2*	0.60 ± 0.06	0.70 ± 0.06	2.6 ± 0.2†
Initial production rate (%/s)	0.49 ± 0.06	0.21 ± 0.04*	0.14 ± 0.02*	0.06 ± 0.02	0.053 ± 0.007	0.31 ± 0.03†
Decay, τ (s)	43 ± 4	35 ± 2	44 ± 4	48 ± 2	33 ± 2†	39 ± 3*

Data are expressed means ± SEM. All metabolite levels, and initial production rates, are expressed as a percentage of maximum [1-^{13}C]pyruvate signal.
Significant difference from pre-ischaemic hearts: *$P < 0.05$ and †$P < 0.001$.

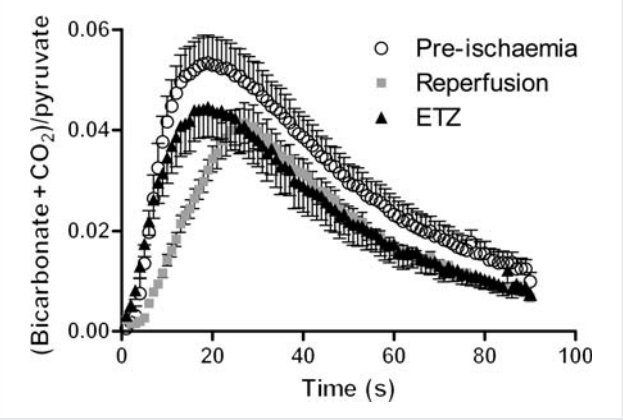

Figure 4 Comparison of the time courses for the sum of the bicarbonate and carbon dioxide peaks, normalized to the maximum value of pyruvate peak area. The maximum peak area did not change following either intervention, compared with the control. Following ischaemia, the initial slope of the curve was significantly reduced.

It is noteworthy that hyperpolarized $H^{13}CO_3^-$ is only a small fraction of total HCO_3^-, and only a minor fraction of transmembrane HCO_3^- efflux would be labelled with hyperpolarized ^{13}C.

Further modelling explored the relationship between pH_i and the steady-state pR (*Figure 7E*) and the time required for equilibration (*Figure 7F*), measured as the time taken for pR to approach steady-state pR within 0.05 U. As CA activity (γ) was increased, steady-state pR approached the true pH_i and did so with a smaller time delay. For low values of CA ($\gamma < 10$), pR significantly underestimated pH_i. Moreover, for values of CA < 10, the time taken for pR to attain steady state was 10–20 s, a significant fraction of the life-time of hyperpolarized ^{13}C compounds[25] and the time of pH_i recovery following ischaemia.

3.5 Measurement of pH_i *in vivo*

A representative spectrum of [1-^{13}C]pyruvate infused *in vivo* is shown in *Figure 8A*. The $H^{13}CO_3^-$ was observed with a signal-to-noise ratio (SNR) of 9.6 ± 1.1, whereas the $^{13}CO_2$ peak had an SNR of 1.2 ± 0.1 and was thus at the limit of detectable signal. Therefore, to calculate pR, 1 s *in vivo* spectra were averaged in groups of two to yield a set of spectra with 2 s temporal resolution and the SNR improved to 16.9 ± 3.5 and 2.0 ± 0.4 for $H^{13}CO_3^-$ and $^{13}CO_2$, respectively. Using the averaged spectra, pR reached a steady-state value of 7.20 ± 0.03, as shown in *Figure 8B*.

4. Discussion

4.1 PDH flux before and after ischaemia

To study the CO_2/HCO_3^- equilibrium, PDH flux must be sufficient to generate MR-detectable levels of $^{13}CO_2$. Therefore, our first aim was to determine the effect of ischaemia on pyruvate oxidation. Others have studied PDH flux upon reperfusion of the ischaemic myocardium, with diverse results depending on the ischaemic model and the perfusion conditions.[17,24,29–31] Kobayashi and Neely[29] observed that pyruvate plus glucose perfusion largely maintained PDH activity in the isolated reperfused heart, and *in vivo* PDH activity was maintained following reduction of coronary flow in swine.[32] However, in the isolated rat heart perfused with pyruvate alone or pyruvate and fatty acids, ischaemia decreased PDH activity and glucose oxidation for several minutes following reperfusion.[17,30,31]

Here, 10 min of total global ischaemia decreased the rate of production of $H^{13}CO_3^-$ plus $^{13}CO_2$ from 0.57 ± 0.06 to 0.26 ± 0.05%/s, indicating a decrease in the initial rate of pyruvate oxidation, and thus inhibition of PDH activity in reperfusion. However, a significant decrease in the total $H^{13}CO_3^-$ and $^{13}CO_2$ produced was not observed, suggesting that PDH flux recovered to control levels within 30 s. Most importantly, sufficient $^{13}CO_2$ was produced at the start of reperfusion to allow the $H^{13}CO_3^-/^{13}CO_2$ ratio to be measured, which, under appropriate conditions, may be used to estimate pH_i.

4.2 CO_2/HCO_3^- equilibrium as a measure of cardiac pH_i

We converted the $H^{13}CO_3^-/^{13}CO_2$ ratio in the isolated perfused rat heart, and in the *in vivo* rat heart, into a variable, pR, using the Henderson–Hasselbalch equation. At steady-state, pR in the isolated perfused rat heart was 7.12 ± 0.1, similar, within the noise inherent in

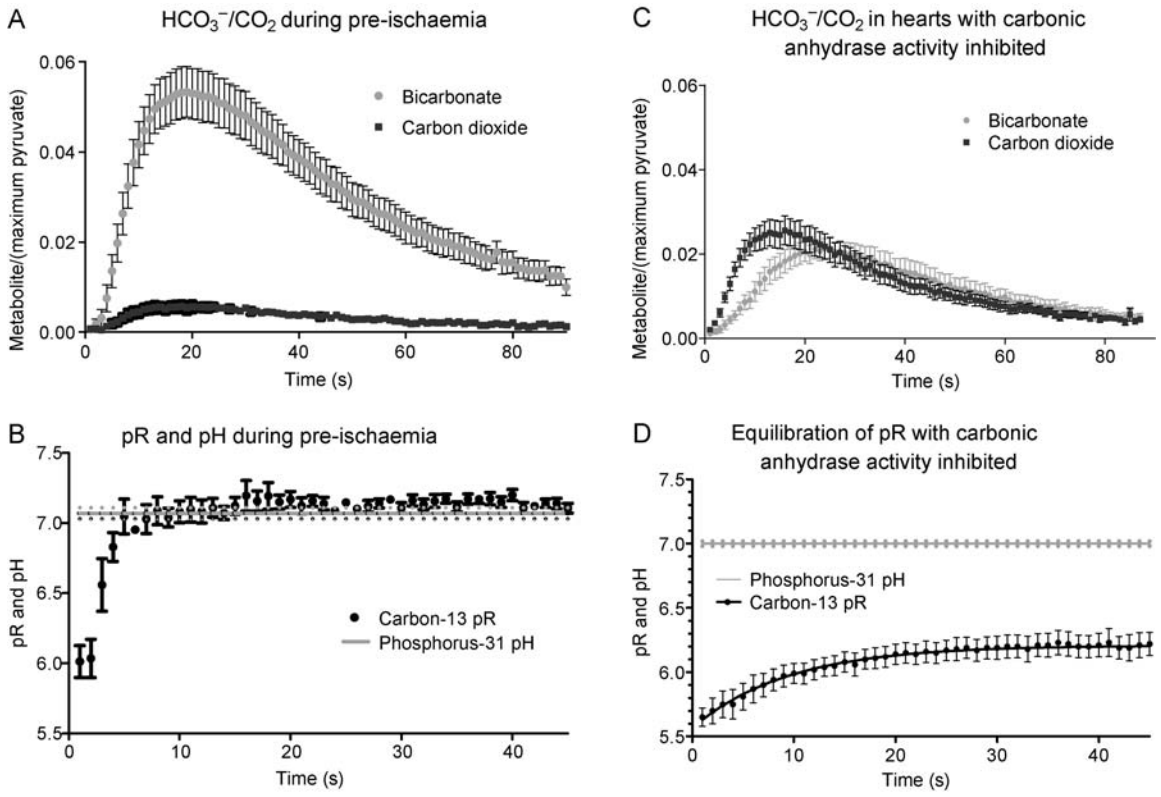

Figure 5 (*A*) The bicarbonate and carbon dioxide, both normalized to maximum pyruvate peak area, vs. time in control hearts ($n = 6$). The point-by-point ratio of these species was used to calculate pR. (*B*) Measurement of pR based on $H^{13}CO_3^-/^{13}CO_2$ in control hearts compared with measurement of pH_i using ^{31}P MRS in the same group of hearts. (*C*) The bicarbonate and carbon dioxide, both normalized to maximum pyruvate peak area, in hearts perfused with the CA inhibitor ETZ ($n = 5$). (*D*) Measurement of pR based on $H^{13}CO_3^-/^{13}CO_2$ in ETZ-perfused hearts compared with measurement of pH_i using ^{31}P MRS in the same group of hearts. The steady-state pR approached 6.21, a value which underestimated the true pH_i of the heart by 0.80 pH units.

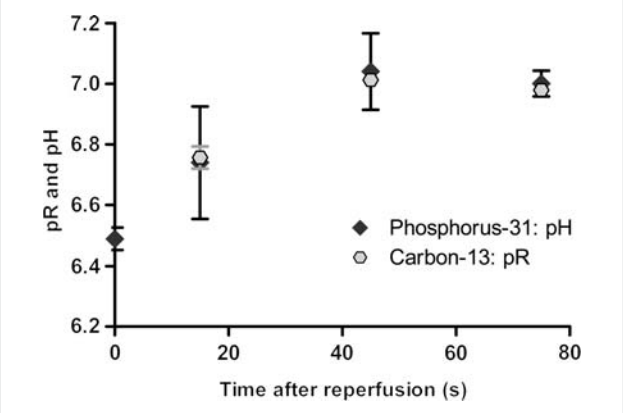

Figure 6 Comparison of the pR measurements made in reperfused hearts using the $H^{13}CO_3^-/^{13}CO_2$ ratio and the pH_i measurements made using ^{31}P MRS. The *x*-axis shows the time after reperfusion with hyperpolarized [1-^{13}C]pyruvate. The ^{31}P measurement at $t = 0$ equals the pH_i following 10 min of simulated ischaemia. Each pR measurement was calculated as the average of 30 s of spectra, acquired 15 s before and after the equivalent ^{31}P measurement to allow for direct comparison.

each measurement, to the pH_i of 7.07 ± 0.02 measured using ^{31}P MRS. When measured in rat hearts *in vivo*, pR was 7.20 ± 0.03. These values are similar to those of Merritt *et al.*,[17] and with pH_i measured by others using ^{31}P MRS.[8–10,20,28] Thus, hyperpolarized [1-^{13}C]pyruvate can be used to obtain an accurate, non-invasive measurement of cardiac pH_i *in vivo* in healthy hearts.[17]

As a first test of the suitability of pR to measure pH_i, we inhibited cardiac CA activity in perfused rat hearts, without altering pH_i. We found a significant difference between the steady-state pR of 6.21 and the pH_i of 7.01 determined using ^{31}P MRS. Low pH_i, such as that observed during myocardial ischaemia, inhibits CA activity.[22,23] Thus, the $H^{13}CO_3^-/^{13}CO_2$ ratio would not be a good measure of pH_i in the ischaemic/reperfused heart without correction for low CA activity.

By modelling our $H^{13}CO_3^-$ and $^{13}CO_2$ results, we identified the conditions in which pR was not a valid measure of pH_i. Provided that sufficient $^{13}CO_2$ is generated via PDH flux, factors that alter the rate of CO_2 production (P_{pyr}, ρ) will not alter steady-state pR. Likewise, CO_2 efflux (P_{CO_2}) does not affect steady-state pR when the heart is perfused to the extent that extracellular $^{13}CO_2$ is washed away rapidly. Changes to CO_2 permeability will alter CO_2 and HCO_3^- levels in parallel and will not affect steady-state pR.

A discrepancy between pR and pH occurred with changes in the rate of CO_2 hydration and events related to HCO_3^- and H^+. The

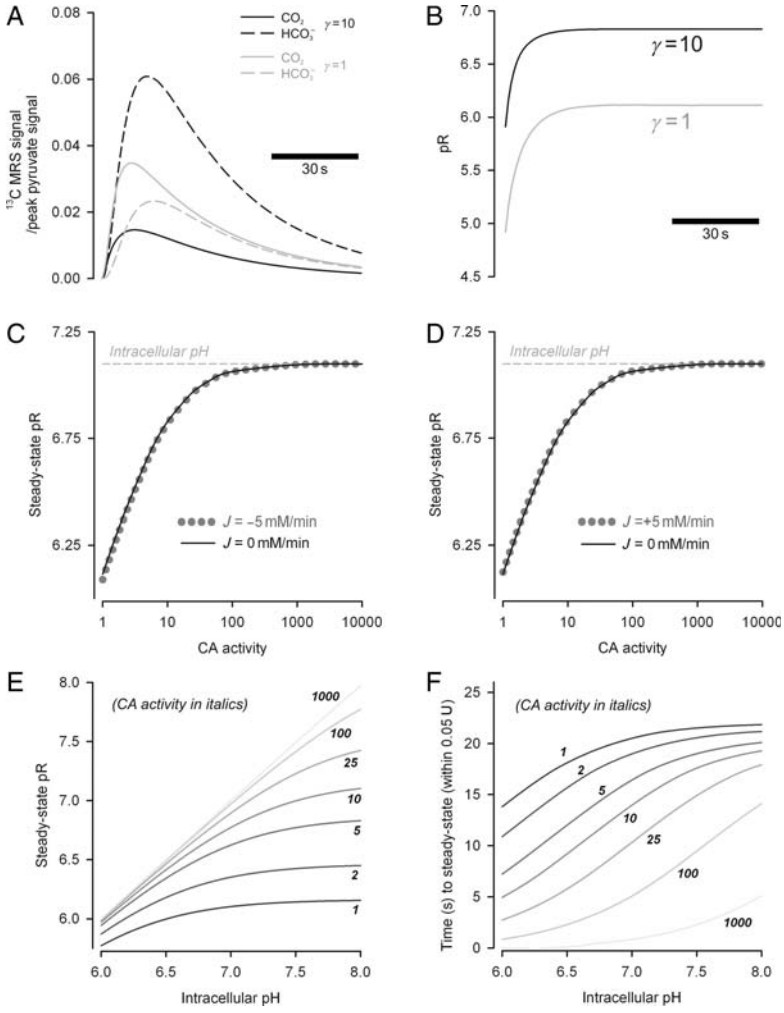

Figure 7 The results of mathematically modelling our experimental data, acquired from control hearts and hearts perfused with ETZ. (*A*) Results from the model which best-fit our experimental data from *Figures 4A* and *5A*. Experimental data were best reproduced with a 10-fold catalytic activity of CA. (*B*) The model simulation of pR, based on the time courses from (*A*). With moderate levels of CA activity, as may be expected in the heart, the $H^{13}CO_3^-/^{13}CO_2$ ratio indicates a steady-state pR that closely approximates the physiological values. However, with lower CA activity, the model reproduced our experimental finding of pH_i underestimation. (*C*) The relationship between CA activity and steady-state pR, in the presence (dashed grey) and absence (black solid) of HCO_3^- efflux or (*D*) influx. CA activity has a significant effect on the size of the pR−pH_i discrepancy, but HCO_3^- transport has a much smaller impact on the discordance. (*E*) Relationship between steady-state pR and pHi, simulated for different levels of CA activity. (*F*) Relationship between equilibration time and pH_i, simulated for different levels of CA activity. Equilibration time was estimated as the time taken for pR to approach steady-state pR within 0.05 U.

rate of CO_2 hydration depends on CA activity. CA activity in cardiac myocytes is modest[21] and, furthermore, CA is inhibited by low pH_i[22,23] and by pharmacological membrane-transport inhibitors.[33] Consequently, CO_2 hydration kinetics have an impact on the suitability of pR as a measure of pH_i. The importance of CA activity was tested using a mathematical model (*Figure 7*). At low CA activity, pR attained a steady-state that could be very different from pH_i, and the equilibration time could be a significant fraction of the lifetime of hyperpolarized ^{13}C or of recovery from ischaemia-induced acidosis.

Membrane transport of H^+ and HCO_3^-, being down-stream of CO_2 hydration, also displaced pR away from pH_i. Because of high pH_i buffering capacity inside myocytes,[2] transport of HCO_3^- would have a relatively greater effect on the state of the CO_2/HCO_3^- equilibrium than H^+ transport. The mathematical model was used to investigate HCO_3^- transport at the modest rate of ± 5 mM/min (*Figure 7C* and *D*). The error due to HCO_3^- transport was, however, negligible and is therefore too slow to significantly affect CO_2/HCO_3^- equilibrium.

4.3 Limitations of the study

To measure pH_i using [1-^{13}C]pyruvate, it is essential that the metabolically generated $H^{13}CO_3^-$ and $^{13}CO_2$ resonances can be accurately quantified above the baseline noise. At a physiological pH of ~7, the $H^{13}CO_3^-$ resonance is 10-fold larger than the $^{13}CO_2$ resonance, so $^{13}CO_2$ quantification requires efficient hyperpolarization, high PDH flux, and careful data acquisition. An increase in achievable polarization, from the ~30% observed here to ~60%, has recently been reported[19] and will aid $^{13}CO_2$ quantification. Also, strategic data acquisition after the ^{13}C equilibration period, over a shorter duration, and with a higher excitation flip angle may further increase the $^{13}CO_2$ signal.

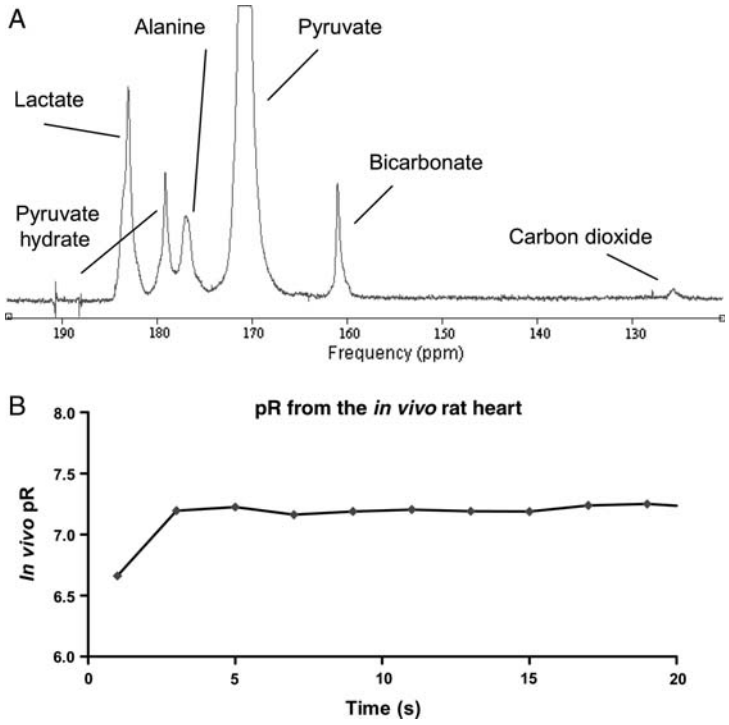

Figure 8 (*A*) Representative *in vivo* spectrum acquired during hyperpolarized [1-^{13}C]pyruvate infusion into living rat hearts. Two single 1 s spectra were summed to yield this spectrum, acquired using a 30° RF pulse. (*B*) Measurement of *in vivo* pR based on $H^{13}CO_3^-/^{13}CO_2$ in living rat hearts.

A second limitation of this study is the fact that the hyperpolarized label cannot directly distinguish between metabolites located in the intra- and extracellular spaces. We can be certain that due to high cardiac oxidative rates, which are more than an order of magnitude higher than any neighbouring tissue (i.e. liver, resting skeletal muscle, adipose tissue, diaphragm, or blood), virtually all of the detected $H^{13}CO_3^-$ and $^{13}CO_2$ signal was produced within the myocardium. However, it is possible that trace amounts of $^{13}CO_2$ may have diffused out of the myocardium and were subsequently hydrated to form $H^{13}CO_3^-$ either spontaneously, by extracellular cardiac CA, or *in vivo*, by CA in red cells. However, we believe that the contribution of the extracellular $H^{13}CO_3^-$ and $^{13}CO_2$ signal to our pH_i measurement was small because: (i) *in vivo* spectroscopic ^{13}C images acquired of the heart[34] have indicated that $H^{13}CO_3^-$ is confined to the myocardium, a region dominated by the intracellular space; (ii) in the perfused heart, high coronary flow rates (~20 mL/min) would have rapidly removed hyperpolarized metabolites, and *in vivo* association of $^{13}CO_2$ with haemoglobin would have caused rapid decay of hyperpolarized MR signal; and (iii) the close agreement between pR measured with ^{13}C and pH_i measured with ^{31}P in the perfused heart indicated minimal contamination from extracellular $H^{13}CO_3^-$ and $^{13}CO_2$, as these species would have equilibrated according the pH_o of 7.4.

4.4 Significance of this work

Currently, the non-invasive measurement of cardiac pH_i in humans is impossible, because blood 2,3-DPG signal overlies the myocardial P_i signal.[6,9,10] Here, we have shown that in the presence of endogenous CA activity, the $H^{13}CO_3^-/^{13}CO_2$ ratio accurately measured pH_i in the isolated perfused heart. Further, we have demonstrated that following infusion of hyperpolarized [1-^{13}C]pyruvate into healthy rats *in vivo*, the MR signal corresponding to $H^{13}CO_3^-$ and $^{13}CO_2$ could both be quantified, and that their ratio indicated a pH_i value of 7.20, which is in line with invasive measurements.[9,10] Consequently, it seems that metabolically generated $H^{13}CO_3^-$ and $^{13}CO_2$ may offer the first technique for the non-invasive measurement of pH_i in normal hearts, and in diseased hearts with normal or elevated CA activity.[35] Measuring *in vivo* pH_i also implies that other analyses of myocardial energetics may be performed *in vivo*, including calculation of free ADP concentrations and the free energy available from the hydrolysis of ATP, ΔG_{ATP}.[5,10] Future work will involve correlating *in vivo* measurements of the $H^{13}CO_3^-/^{13}CO_2$ ratio with pH_i measurements made using invasive, blood-removed or open-chest techniques.[9,10]

Since acidosis is a characteristic feature of ischaemia, assessment of ischaemic heart disease in humans is another potentially useful application of a non-invasive pH_i calculation using the $H^{13}CO_3^-/^{13}CO_2$ ratio. We observed excellent agreement between pH_i measured using ^{31}P MRS and pR measured using ^{13}C MRS in the reperfused myocardium when pH_i was $\geq$6.74 (*Figure 6*). However, multiple factors shift pR relative to pH_i, including inhibition of CA activity at low pH_i[22,23] and stimulation of membrane transport during reperfusion following ischaemia.[2,36] Pharmaceutical agents, such as cariporide, inhibit membrane ion transport and have been used clinically to reduce ischaemia–reperfusion injury,[37] but also block CA.[33] Therefore, the use of the $H^{13}CO_3^-/^{13}CO_2$ ratio to measure pH_i may not be valid in ischaemic, acidic hearts, and in patients with ischaemic heart disease who use drugs that inhibit membrane ion transport. Additionally, it is reasonable to expect that intracellular CA expression and activity may be either reduced or increased in other forms of cardiomyopathy.[35] Correction of pR to pH_i will require

full characterization of CA activity in each pathophysiological state, and mathematical deconvolution of the ^{13}C equilibration period from the true measured pH_i changes.

Eventual translation of the $H^{13}CO_3^-/^{13}CO_2$ ratio to measure pH_i in the clinic will require considerable technological advances, in terms of improved methods and hardware for acquisition of ^{13}C images, and access to affordable hyperpolarization tools and ^{13}C-labelled compounds. In order to identify focal regions of ischaemia using pH_i measurements from hyperpolarized [1-^{13}C]pyruvate, for example, three-dimensional images of $H^{13}CO_3^-$ and $^{13}CO_2$ with relatively high spatial resolution across the area at risk will be required. The feasibility of acquiring such data across the myocardium of large animals, and therefore patients, has been demonstrated.[34] Further, although the eventual cost of clinical application of the hyperpolarized ^{13}C MR technology is not clear, it does not appear set to be prohibitive. Clinical polarizers could be operated as standalone systems, placed within existing clinical MR facilities and interfaced to existing MR scanners. Further, the cost of [1-^{13}C]pyruvic acid, as used here, is not excessive and would be in line with contrast agents used in other imaging modalities, such as positron emission tomography.

In summary, we have demonstrated in the perfused heart that the $H^{13}CO_3^-/^{13}CO_2$ ratio offers an accurate method to measure cardiac pH_i in hearts with normal or elevated CA activity. Further, the technique appears set to become the first clinically relevant measure of *in vivo* cardiac pH_i, although future work is warranted to characterize CA activity and the response of the $H^{13}CO_3^-/^{13}CO_2$ ratio in ischaemia and other cardiomyopathies, and to improve the sensitivity and spatial resolution of $H^{13}CO_3^-$ and $^{13}CO_2$ detection.

Supplementary material

Supplementary material is available at *Cardiovascular Research* online.

Acknowledgements

The authors would like to thank Prof. Richard Vaughan-Jones, Prof. Kevin Brindle, and Dr Jan-Henrik Ardenkjær-Larsen for helpful suggestions.

Conflict of interest: This work received research support from GE-Healthcare.

Funding

M.A.S. is funded by the Newton Abraham Scholarship Foundation, NIH grant no. 1-F31-EB006692-01A1 and the Wellcome Trust. P.S. is funded by the Medical Research Council and the Royal Society. F.A.G. is funded by Cancer Research UK and the National Institute of Health Research Cambridge Biomedical Research Centre. This work was funded by grants from the Medical Research Council (MRC Grant G0601490) and the British Heart Foundation (BHF Grant PG/07/070/23365), and by GE-Healthcare. Funding to pay the Open Access publication charges for this article was provided by the Wellcome Trust.

References

1. Garlick PB, Radda GK, Seeley PJ. Studies of acidosis in the ischaemic heart by phosphorus nuclear magnetic resonance. *Biochem J* 1979;**184**:547–554.
2. Vaughan-Jones RD, Spitzer KW, Swietach P. Intracellular pH regulation in heart. *J Mol Cell Cardiol* 2009;**46**:318–331.
3. Opie LH. Myocardial ischemia–metabolic pathways and implications of increased glycolysis. *Cardiovasc Drugs Ther* 1990;**4**(Suppl. 4):777–790.
4. Bing OH, Brooks WW, Messer JV. Heart muscle viability following hypoxia: protective effect of acidosis. *Science* 1973;**180**:1297–1298.
5. Ingwall J. *ATP and the Heart*. Boston: Kluwer Academic Publishers; 2002.
6. Frohlich O, Wallert MA. Methods of measuring intracellular pH in the heart. *Cardiovasc Res* 1995;**29**:194–202.
7. Hoult DI, Busby SJ, Gadian DG, Radda GK, Richards RE, Seeley PJ. Observation of tissue metabolites using ^{31}P nuclear magnetic resonance. *Nature* 1974;**252**:285–287.
8. Bailey IA, Williams SR, Radda GK, Gadian DG. Activity of phosphorylase in total global ischaemia in the rat heart. A phosphorus-31 nuclear-magnetic-resonance study. *Biochem J* 1981;**196**:171–178.
9. Katz LA, Swain JA, Portman MA, Balaban RS. Intracellular pH and inorganic phosphate content of heart *in vivo*: a ^{31}P-NMR study. *Am J Physiol* 1988;**255**:H189–H196.
10. Brindle KM, Rajagopalan B, Williams DS, Detre JA, Simplaceanu E, Ho C *et al*. P-31 NMR measurements of myocardial pH *in vivo*. *Biochem Biophys Res Commun* 1988;**151**:70–77.
11. Gallagher FA, Kettunen MI, Day SE, Hu DE, Ardenkjaer-Larsen JH, Zandt R *et al*. Magnetic resonance imaging of pH *in vivo* using hyperpolarized ^{13}C-labelled bicarbonate. *Nature* 2008;**453**:940–943.
12. Leem CH, Lagadic-Gossmann D, Vaughan-Jones RD. Characterization of intracellular pH regulation in the guinea-pig ventricular myocyte. *J Physiol* 1999;**517**:159–180.
13. Swietach P, Vaughan-Jones RD, Harris AL. Regulation of tumor pH and the role of carbonic anhydrase 9. *Cancer Metastasis Rev* 2007;**26**:299–310.
14. Hoffman DW, Henkens RW. The rates of fast reactions of carbon dioxide and bicarbonate in human erythrocytes measured by carbon-13 NMR. *Biochem Biophys Res Commun* 1987;**143**:67–73.
15. Madshus IH. Regulation of intracellular pH in eukaryotic cells. *Biochem J* 1988;**250**:1–8.
16. Merritt ME, Harrison C, Storey C, Jeffrey FM, Sherry AD, Malloy CR. Hyperpolarized 13C allows a direct measure of flux through a single enzyme-catalyzed step by NMR. *Proc Natl Acad Sci USA* 2007;**104**:19773–19777.
17. Merritt ME, Harrison C, Storey C, Sherry AD, Malloy CR. Inhibition of carbohydrate oxidation during the first minute of reperfusion after brief ischemia: NMR detection of hyperpolarized $^{13}CO_2$ and $H^{13}CO_3$. *Magn Reson Med* 2008;**60**:1029–1036.
18. Schroeder M, Cochlin L, Heather L, Clarke K, Radda G, Tyler D. *In vivo* assessment of pyruvate dehydrogenase flux in the heart using hyperpolarized carbon-13 magnetic resonance. *Proc Natl Acad Sci USA* 2008;**105**:12051–12056.
19. Johannesson H, Macholl S, Ardenkjaer-Larsen JH. Dynamic nuclear polarization of [1-^{13}C]pyruvic acid at 4.6 tesla. *J Magn Reson* 2009;**197**:167–175.
20. Vandenberg JI, Carter ND, Bethell HW, Nogradi A, Ridderstrale Y, Metcalfe JC *et al*. Carbonic anhydrase and cardiac pH regulation. *Am J Physiol* 1996;**271**:C1838–C1846.
21. Leem CH, Vaughan-Jones RD. Out-of-equilibrium pH transients in the guinea-pig ventricular myocyte. *J Physiol* 1998;**509**:471–485.
22. Kernohan JC. The pH-activity curve of bovine carbonic anhydrase and its relationship to the inhibition of the enzyme by anions. *Biochim Biophys Acta* 1965;**96**:304–317.
23. Khalifah RG. The carbon dioxide hydration activity of carbonic anhydrase. I. Stop-flow kinetic studies on the native human isoenzymes B and C. *J Biol Chem* 1971;**246**:2561–2573.
24. Schroeder MA, Atherton HJ, Ball DR, Cole MA, Heather LC, Griffin JL *et al*. Real-time assessment of Krebs cycle metabolism using hyperpolarized ^{13}C magnetic resonance spectroscopy. *FASEB J* 2009;**23**:2529–2538.
25. Ardenkjaer-Larsen JH, Fridlund B, Gram A, Hansson G, Hansson L, Lerche MH *et al*. Increase in signal-to-noise ratio of >10,000 times in liquid-state NMR. *Proc Natl Acad Sci USA* 2003;**100**:10158–10163.
26. Naressi A, Couturier C, Castang I, de Beer R, Graveron-Demilly D. Java-based graphical user interface for MRUI, a software package for quantitation of *in vivo*/medical magnetic resonance spectroscopy signals. *Comput Biol Med* 2001;**31**:269–286.
27. Murray AJ, Lygate CA, Cole MA, Carr CA, Radda GK, Neubauer S *et al*. Insulin resistance, abnormal energy metabolism and increased ischemic damage in the chronically infarcted rat heart. *Cardiovasc Res* 2006;**71**:149–157.
28. Cross HR, Clarke K, Opie LH, Radda GK. Is lactate-induced myocardial ischaemic injury mediated by decreased pH or increased intracellular lactate? *J Mol Cell Cardiol* 1995;**27**:1369–1381.
29. Kobayashi K, Neely JR. Effects of ischemia and reperfusion on pyruvate dehydrogenase activity in isolated rat hearts. *J Mol Cell Cardiol* 1983;**15**:359–367.
30. Lewandowski ED, White LT. Pyruvate dehydrogenase influences postischemic heart function. *Circulation* 1995;**91**:2071–2079.
31. Lopaschuk GD, Spafford MA, Davies NJ, Wall SR. Glucose and palmitate oxidation in isolated working rat hearts reperfused after a period of transient global ischemia. *Circ Res* 1990;**66**:546–553.
32. Stanley WC, Hernandez LA, Spires D, Bringas J, Wallace S, McCormack JG. Pyruvate dehydrogenase activity and malonyl CoA levels in normal and ischemic swine myocardium: effects of dichloroacetate. *J Mol Cell Cardiol* 1996;**28**:905–914.
33. Villafuerte FC, Swietach P, Vaughan-Jones RD. Common inhibitors of membrane H^+-transport also inhibit carbonic anhydrase. *FASEB J* 2007;**21**:A1284–A1284.
34. Golman K, Petersson JS, Magnusson P, Johansson E, Akeson P, Chai CM *et al*. Cardiac metabolism measured noninvasively by hyperpolarized ^{13}C MRI. *Magn Reson Med* 2008;**59**:1005–1013.
35. Alvarez BV, Johnson DE, Sowah D, Soliman D, Light PE, Xia Y *et al*. Carbonic anhydrase inhibition prevents and reverts cardiomyocyte hypertrophy. *J Physiol* 2007;**579**:127–145.
36. Vandenberg JI, Metcalfe JC, Grace AA. Mechanisms of pHi recovery after global ischemia in the perfused heart. *Circ Res* 1993;**72**:993–1003.
37. Scholz W, Albus U, Counillon L, Gogelein H, Lang HJ, Linz W *et al*. Protective effects of HOE642, a selective sodium-hydrogen exchange subtype 1 inhibitor, on cardiac ischaemia and reperfusion. *Cardiovasc Res* 1995;**29**:260–268.